一般セッション(口頭講演) | 4 JSAP-Optica Joint Symposia 2024：4.3 Laser sources and Laser applications

2024年9月17日(火) 10:45 ~ 12:00 A31 (朱鷺メッセ3F)

[17a-A31-1~5] 4.3 Laser sources and Laser applications

Set Sze Yun(東大)

英語発表
10:45 ~ 11:00
[17a-A31-1]
3D Reconstruction of Veins Using NIR by Efficientnet Model

Phuong Anh Dam[1], ○(M1)Hoang Nhut Huynh[1], Tan Loc Huynh[1], Kien Vinh Vuong[1], Ngoc An Dang Nguyen[1], Anh Tu Tran[1], Trung Nghia Tran[1] (1.Ho Chi Minh City University of Technology (HCMUT), VNUHCM)

英語発表
11:00 ~ 11:15
[17a-A31-2]
An Optical Approach for the Liquid Vortex Characterization

○(M1)Tien Danh Vu[1,2], Phuong Hoang Le[1], Thanh Nhu Nguyen[1,2], Binh Xuan Cao[1,2] (1.Square Lab, Hanoi University of Science and Technology, 2.School of Mechanical Engineering, Hanoi University of Science and Technology)

英語発表
11:15 ~ 11:30
[17a-A31-3]
Utilizing Near-Infrared Femtosecond Laser-Generated Gas Bubbles for Acellular Area Construction in Cell Monolayers

○Kazunori Okano[1,4], Naomi Tanga[1,2], Rieko Aida[4], Hayato Suwa[4], Hiromi Hagiwara[4], Yalikun Yaxiaer[1], Koichiro Kishima[5], Yoichiroh Hosokawa[1,2,3] (1.Mat. Sci, NAIST, 2.CDG, NAIST, 3.MediLux, NAIST, 4.Toin Yokohama Univ., 5.Pinpoint Photonics)

英語発表
11:30 ~ 11:45
[17a-A31-4]
Evaluating Single Event Effects in Radiation-Tolerant Chips Using Short-Pulse Laser

○(M2)Chien Ping Hung[1], Shih Bo Yu[1], Jia Han Li[1] (1.National Taiwan Univ)

英語発表
11:45 ~ 12:00
[17a-A31-5]
【No-Show】BREAKING OF PHONON BOTTLENECK IN $CsPbI_3$ NANOCRYSTALS DUE TO EFFICIENT AUGER RECOMBINATION

○(D)Ankit Sharma[1], Samit K Ray[2], K V Adarsh[1] (1.IISER Bhopal India, 2.IIT Kharagpur India)

3D Reconstruction of Veins Using NIR by Efficientnet Model

Phuong Anh Dam[1,2], Hoang Nhut Huynh[1,2], Tan Loc Huynh[1,2], Kien Vinh Vuong[1,2], Ngoc An Dang Nguyen[1,2], Anh Tu Tran[1,2], and Trung Nghia Tran[1,2]

[1] Laboratory of Laser Technology, Faculty of Applied Science, Ho Chi Minh City University of Technology (HCMUT), 268 Ly Thuong Kiet Street, District 10, Ho Chi Minh City 72409, Vietnam,
[2] Vietnam National University Ho Chi Minh City, Linh Trung Ward, Thu Duc, Ho Chi Minh City 71308, Vietnam
E-mail: ttnghia@hcmut.edu.vn

1. Introduction

The study proposed a method for visualizing veins using near-infrared (NIR) transillumination imaging and reconstructing 3D structures with an EfficientNet CNN model and pixel-to-pixel technique. NIR imaging, despite being noninvasive, encounters issues with light scattering, resulting in blurry images with poor depth perception. The proposed method combines depth estimation and scatter deblurring to improve the clarity and accuracy of 3D reconstructions, specifically targeting veins on the back of the hand.

2. Method

The methodology for 3D vein reconstruction using NIR imaging and deep learning involves an image acquisition system that captures NIR images of hand vascular structures. Depth estimation and scatter deblurring are performed with an EfficientNet CNN model and pixel-to-pixel method. This includes preparing training data with blurred NIR images and corresponding depth maps, training the model to predict pixel depths, and generating a Depth Estimation Matrix (DEM) as shown in Figure 1.

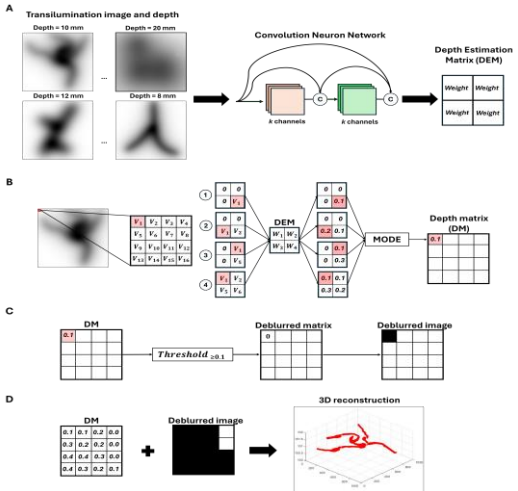

Figure 1. A. Depth estimation method, training data includes blurred images and depth, B. pixel-by-pixel method, C. deblurring method using depth matrix and depth thresholding, and D. reconstructing 3D structure from deblurred image and depth matrix.

The pixel-to-pixel method improves depth estimation by scanning the image, applying zero padding, and selecting the most common depth for each pixel. Scatter deblurring enhances clarity by using a depth threshold on the DEM, generating a deblurred image, and reconstructing the 3D structure using depth values on the x-y and z axes.

The model is trained with 100,000 images, a depth range of 0.1 to 50.0 mm, a batch size of 8, over 50 epochs, using the Adam optimizer and accuracy as the metric. Experiments, including simulations and real tissue tests capturing NIR images of the hand, show that the model effectively improves image clarity and depth estimation, leading to accurate 3D reconstructions of vascular structures as shown in Figure 2.

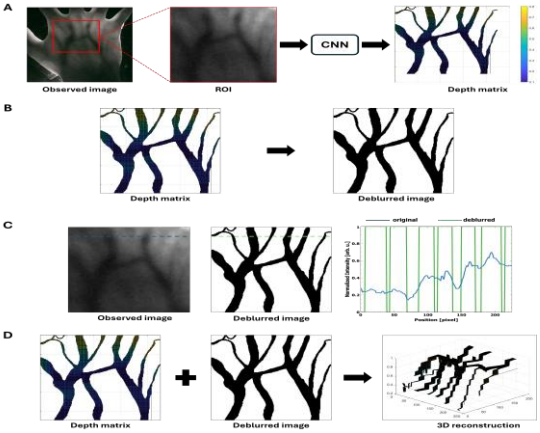

Figure 2. 3D reconstruction results of blood vessels using CNN model with A. Extracting ROI and estimating depth with CNN, B. Applying a depth matrix threshold to obtain a deblurred image, C. Comparing intensity profiles of observed and deblurred images, and D. Reconstructing the 3D blood vessel structure from the depth matrix and deblurred image.

3. Conclusion

The study proposed approach enhances 3D vein reconstruction through NIR imaging with the EfficientNet model and the pixel-to-pixel method, improving image clarity and depth estimation. Experimental results verify its accuracy and potential for noninvasive biomedical imaging, especially in vascular diagnostics and monitoring.

Acknowledgements

We acknowledge Ho Chi Minh City University of Technology (HCMUT), VNU-HCM for supporting this study

References

[1] M. Tan and Q. Le, “Efficientnet: Rethinking model scaling for convolutional neural networks,” in *International conference on machine learning*, pp. 6105–6114, PMLR, 2019.
[2] N. A. Dang Nguyen et al. “Improvement of the performance of scattering suppression and absorbing structure depth estimation on transillumination image by deep learning,” Applied Sciences, vol. 13, no. 18, p. 10047, 2023.

An Optical Approach for the Liquid Vortex Characterization

Tien Danh Vu[1,2], Phuong Le Hoang[1], Thanh Nhu Nguyen[1,2], Binh Xuan Cao[1,2]

[1] Square Lab, Hanoi University of Science and Technology, Hanoi 100000, Viet Nam,
[2] School of Mechanical Engineering, Hanoi University of Science and Technology, Hanoi 100000, Viet Nam
E-mail: binh.caoxuan@hust.edu.vn

1. Introduction

Research on liquid vortices is integral to fluid mechanics and is applied in various fields, including the manufacturing of optical elements [1]. To discover liquid vortex surfaces, contact methods [2], though simple, damage surface structures. Noncontact methods offer high-speed and accurate measurements but require complex systems [3]. Most experimental setups are suboptimal.

This paper proposes a straightforward approach combining the optical system and image processing techniques to investigate liquid vortex surfaces by light reflection. Collimated laser beams directed onto liquid surfaces provide vortex parameters through reflected beam profile analysis. The method is validated by the parabolic shape of liquid vortices in a rotary cylinder, showing promise for liquid characterization using simple optical elements.

2. Experimental Method

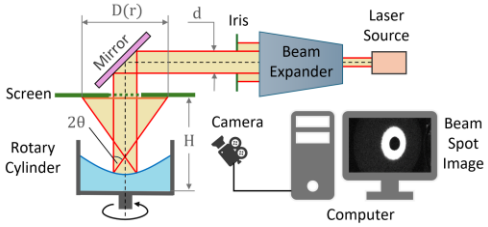

Figure 1 Experiment Setup

Liquid vortices are examined in real-time through surface reflection. The axially symmetric liquid surface is described by $z = z(r)$. A collimated, expanded laser beam shines perpendicular to the rotating liquid surface, with its axis aligned with the rotation axis. An iris diaphragm creates various beam radii, and the diameter of the incoming beam d equals the iris aperture. The reflected beam profile is recorded with its spot width monitored by a camera with image processing techniques and an observation screen with a central hole for the collimated beam. The optical path of two symmetric boundary rays of the collimated beam is illustrated in Fig. 1. Given the tangent slope at the reflection point is θ, the angle between reflected and incoming beams is 2θ. The beam width on the screen $D(r)$ is calculated:

$$D(r) = 2\left(H - z\right)\tan(2\theta) - d = 4z'\left(H - z\right)\left(1 - z'^{2}\right)^{-1} - 2r \quad (1)$$

where r is the incident beam radius $(r = d/2)$, and H is the distance from the cylinder bottom to the observation screen. A rotatable cylindrical liquid container driven by a rotor is precisely controlled by the encoder feedback signal with a PID controller. When the container rotates with liquid inside, it creates vortices.

3. Results and Discussion

The following parameters were investigated in this study. Two 150 ml liquid samples were used in the experiment including a saline solution (NaCl; 0.9) and a propylene glycol solution ($C_3H_8O_2$; 99). The viscosities of the saline and glycol solutions, at standard experimental conditions (25°C, 1 atm), are 0.9 cp and 57 cp, respectively, and their approximate densities are 1 mg/l. The container angular velocity is 15 ± 0.12 rad/s. The iris aperture is adjusted to investigate incident beam diameters in the range of 10─19 mm.

The parabolic shape of the liquid vortex surface has been demonstrated in previous research [1,2]. Initial results with 10 incident beam diameters for both solutions show similar vortex surface profiles by the data on reflected beam spots. A detailed analysis with 37 iris aperture values further examines the relationship between the reflected spot size and the incoming beam radius $D(r)$, described as a quadratic function of $z(r)$ (Eq. 3). The vortex surface shape, as determined by fitting the plots, closely matches a parabola, with $R^2 \geq 99\%$. The proposed method effectively investigates liquid vortices.

4. Conclusion

This method analyzes liquid vortices by light reflection. A collimated laser beam directed onto liquid surfaces determines vortex parameters from reflected beam data. Studying vortices in a rotating cylinder with propylene glycol and saline solutions at 15 rad/s, we determine similar vortex shapes. Curve fitting shows the vortex surface is nearly parabolic. The method offers a technique to characterize liquid dynamics.

References

[1] Wattinger, M., Gordon, P., Ghorayshi, M. & Coté, G. Method and system for the centrifugal fabrication of low cost, polymeric, parabolic lenses. Opt Express 27, 21405 (2019).
[2] Menker, P. & Herczyński, A. Form of spinning liquids in diverse geometries. Am J Phys 88, 475–482 (2020).
[3] Arshad, M., Rowland, E. M., Riemer, K., Sherwin, S. J. & Weinberg, P. D. Improvement and validation of a computational model of flow in the swirling well cell culture model. Biotechnol Bioeng 119, 72–88 (2022).

Utilizing Near-Infrared Femtosecond Laser-Generated Gas Bubbles for Acellular Area Construction in Cell Monolayers

Kazunori Okano[1,4], Naomi Tanga[1,2], Rieko Aida[4], Hayato Suwa[4], Hiromi Hagiwara[4], Yalikun Yaxiaer[1], Koichiro Kishima[5], Yoichiroh Hosokawa[1,2,3]

[1] Division of Materials Science, Nara Institute of Science and Technology. [2] Center for Digital Green-innovation, Nara Institute of Science and Technology, [3] MediLux Research Center, Nara Institute of Science and Technology, [4] Faculty of Biomedical Engineering, Toin Yokohama University, [5] Pinpoint Photonics, Inc.
E-mail: k-okano@ms.naist.jp

The focused irradiation of near-infrared femtosecond laser (NIR fs laser) pulses in biological solvents efficiently induces molecular breakdown, generating vaporous gas micro bubbles [1]. Such irradiation on live cells induces apoptosis and necrosis depending in pulse energy [2]. Here we examined the relation bubble size and numbers and pulse energy in cells. Further, the NIR fs laser bubbling-formed cell-removed acellular area was used for assaying antimotility effects of the plant flavonoid apigenin.

Gas bubble generation

An acellular rectangular area was pre-formed by NIR fs laser scanning (Fig. 1). The same laser was then scanned across the cell monolayer at a right angle, intersecting the acellular region. The gas bubble observed at cell monolayer area while no bubbles at acellular area, indicating that required pulse energy for the bubble generation was different at live cell and medium.

Series of experiments at different energy condition estimated that pulse energy threshold was 35 and 80 nJ for cell monolayer and medium, respectively (Fig. 2). The pulse irradiation condition ranging from 30 to 80 nJ could ablate cells without medium bubbling. The bubbles remained in cells for several to more than 10 s at 100 nJ pulse irradiation while immediate decayed at irradiation to medium. Below 30 nJ, gas bubbles were never generated, and cells receive no lethal damage. Above 80 nJ, the bubbles vigorously generated in both cells and medium.

Application in biology

The NIR fs laser-based bubbling was employed to demonstrate its effectiveness in evaluating the motility of a lung cancer cell line A549, particularly in the context of assessing the antimotility effects of the plant flavonoid apigenin (Fig. 3). The acellular area closed completely within 6 h in the regular medium, whereas in the apigenin containing medium, it persisted beyond the 6 h mark. Quantitative analysis revealed a significant and dose-dependent reduction in the motility rate of A549 cells with apigenin treatment. The 50% effective apigenin concentration (ED50) was observed at 60 μM.

Methods

A549 cell line (RCB3677) was cultured in DMEM containing 9% FBS and antibiotics until making cell monolayer on a glass-bottom dish. NIR fs laser ablation (800 nm, 1 kHz) was executed at a speed of 600 μm/s over an area of 50 × 250 μm. The laser pulse energy was measured with a laser power meter after the objective lens. Throughout the laser scanning process, bubble generation and cell monolayer conditions were recorded with a CMOS camera.

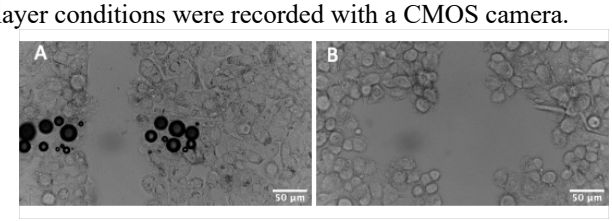

Fig. 1 Bright field micrographs of A549 cell monolayer (A) during and (B) after NIR fs laser scanning (60 nJ).

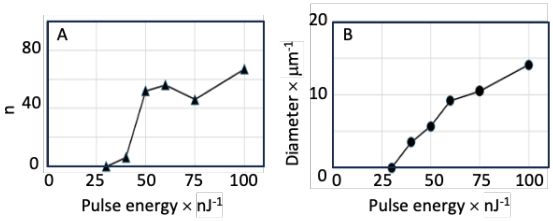

Fig. 2 Pulse energy response of micro bubbles generation in a cell monolayer. Number of bubbles (A) and bubble diameter (B) vs. pulse energy.

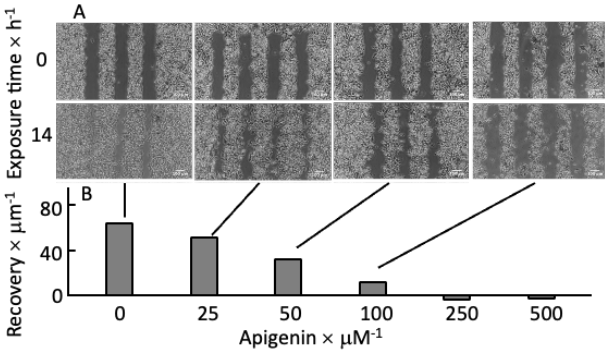

Fig. 3 Apigenin dose response in acellular area recovery. Micrographs before and 14 h after apigenin treatment (A) and the width of recovery area after 14 h of treatment (B).

Acknowledgements

This study was supported with Pinpoint Photonics, Inc.

References

[1] R. Yasukuni, A. Koyanagi, Y. Tanaka, K. Okano, Y.Hosokawa, Sci. Rep. **12** 19001 (2022).
[2] K. Okano, C.-H. Wang, Z.-Yi Hong, Yoichiroh Hosokawa, Ian Liau, Biochem. Biophys. Res. **24** 199817 (2020).

Evaluating Single Event Effects in Radiation-Tolerant Chips Using Short-Pulse Laser

Chien-Ping Hung, Shih-Bo Yu, and Jia-Han Li*

Department of Engineering Science and Ocean Engineering, National Taiwan University, Taipei 10617, Taiwan

Email: R11525065@ntu.edu.tw, R10525092@ntu.edu.tw, *: jiahan@ntu.edu.tw

1. Introduction

Radiation-tolerant chips are essential for high-reliability applications in aerospace, military, and nuclear industries, as they withstand high radiation levels without performance degradation. Short pulse lasers are used to test these chips, offering high precision and the ability to simulate various radiation effects in a controlled setting, providing valuable insights into their performance and reliability.

We test radiation-tolerant chips using 800 nm and 1060 nm lasers. Each wavelength interacts differently with the chip's material, allowing for a comprehensive analysis of their behavior under diverse conditions. This approach identifies the strengths and weaknesses of different circuit designs and materials. Additionally, these lasers can induce Single Event Effects (SEE) in the chips, enabling further analysis of their vulnerability and resilience.

2. Method

Our short-pulse laser platform involves two laser sources operating at wavelengths of 800 nm and 1060 nm, each with varying camera modules. Because the 1060 nm laser spectrum is entirely in the non-visible range, it is necessary to use an IR camera module to observe the irradiation position.

The figure below shows a block diagram of the experimental setup, detailing the different modules within the system.

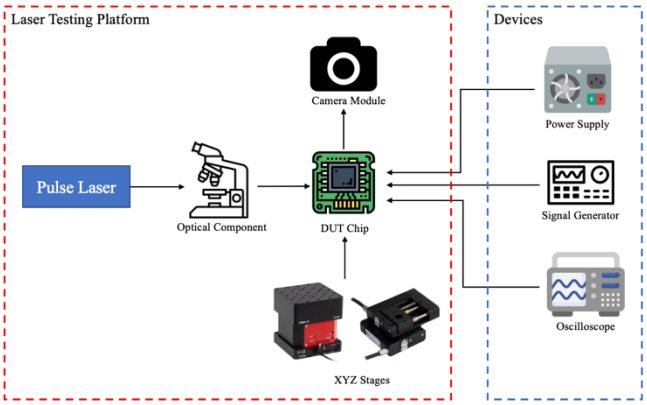

Figure 1. Block Diagram of Laser Testing Platform [1][2]

Objective of each experiment is to detect SEE in each DUT, which includes identifying SET (Single Event Transient), SEU (Single Event Upset), or bit errors in the memory. Next, based on the different DUTs, we analyze the data to assess their radiation resistance and identify sensitive areas.

3. Results and Discussion

The current optical path structure used in the experiments maintains a laser spot size of approximately 5 µm. This fine spot size, combined with a minimum step size of 50 nm on the moterized platform, is essential for high-resolution scanning and accurate detection of radiation effects on the chip.

The scanning path used in the experiments follows established protocols, ensuring that the entire chip surface is systematically scanned. [3]

The analysis of irradiation results includes both front and back illumination scenarios. The observed SEE in these experiments are documented and compared. The findings indicate that the proportion of sensitive areas relative to the entire chip is very small, underscoring the importance of precise positioning and scanning during the tests.

4. Conclusions

The experiments demonstrate that both 800 nm and 1060 nm lasers can induce SEE in the DUT. However, it is noted that the 1060 nm laser is more suitable for back illumination experiments, likely due to its higher penetration rate compared to the 800 nm laser. [4]

The cross-section analysis of the chip can be compared with particle experiments to validate the findings. This comparison provides a more comprehensive understanding of the chip's behavior under different radiation conditions.

Additionally, the bit error rate (BER) for memory components within the chip is analyzed for its correlation with the observed SEE. This analysis helps assess the overall reliability of the memory under radiation exposure and guides the design of more robust radiation-tolerant chips.

Acknowledgements

This research was funded by the Ministry of Science and Technology of Taiwan MOST 113-NU -E-002 -001 -NU, and financial support and technical support from the Taiwan Space Agency and Nuclear Safety Commission.

References

[1]https://www.thorlabs.com/thorproduct.cfm?partnumber=KVS0
[2]https://www.physikinstrumente.com/en/products/linear-stages/stages-with-stepper-dc-brushless-dc-bldc-motors/m-110-m-111-m-112-compact-linear-stage-412418433
[3] Lei, Zhifeng, et al. "Single Event Effects test for CMOS devices using 1064nm pulsed laser." 2011 International Conference on Quality, Reliability, Risk, Maintenance, and Safety Engineering. IEEE, 2011.
[4] Buchner, Stephen P., et al. "Pulsed-laser testing for single-event effects investigations." IEEE Transactions on Nuclear Science60.3 (2013): 1852-1875.

BREAKING OF PHONON BOTTLENECK IN $CsPbI_3$ NANOCRYSTALS DUE TO EFFICIENT AUGER RECOMBINATION

Ankit Sharma*[1], Samit K Ray[2], K V Adarsh*[1]

[1] *Department of Physics, Indian Institute of Science Education and Research, Madhya Pradesh, India, 462066*

[2] *Department of Physics, Indian Institute of Technology Kharagpur, West Bengal, India, 721302,*

Email id: ankits19@iiserb.ac.in and adarsh@iiserb.ac.in

ABSTRACT

Inorganics lead halide perovskite (LHP) have been became appropriate system for demonstrating light-matter interaction due to their flexible bandgap tunability, defect tolerance and high photoluminescence quantum yield nature. Although, LHPs have many hallmark properties which can support highly efficient photovoltaic devices, but they lost lot of energy in carriers-phonon scattering which slow down the recombination process and decrease the efficiency. Faster thermalization time of hot carriers support electron-hole recombination at band-edge which can be exploited in optoelectronic devices either by incorporating electrons/holes transport layer for photovoltaic or fast recombination for LED. Recently, efficient photovoltaic and light emitting devices are immediate requirement for high-speed quantum technologies. Here, we have chosen $CsPbI_3$ and Cu-doped $CsPbI_3$ nanocrystals (NCs) and addressed both issues simultaneously by using transient absorption spectroscopy. Our sample can be classified as an intermediate confinement as the size of NCs is 16 nm (32 nm) for $CsPbI_3$ (Cu-doped $CsPbI_3$) NCs which are higher than Bohr's radius (~12 nm), and give sharp excitonic peaks in ground state optical absorption with excitonic position at ~2.1 eV. Further, by femtosecond laser excitation with 400 nm and 120 fs pulse width, which is generated by second harmonic of fundamental wavelength 800 nm. The fluence-dependent measurement revealed the many-body interaction and hot carriers dynamics. At higher fluence, say 150 $\mu J/cm^2$ and above, pristine $CsPbI_3$ NCs shows breaking of phonon bottleneck effect by fast decay while Cu-doped NCs showed slow thermalization. To get insight, we have calculated Auger recombination (non-radiative) lifetime by subtractive method. The lifetime measurements clearly distinguished the appearance of contrast results due to efficient Auger process associated with pristine $CsPbI_3$ NCs. Thus, our results provide insight to incorporate metal doping and understanding about hot carrier dynamics for solar energy harvesting.

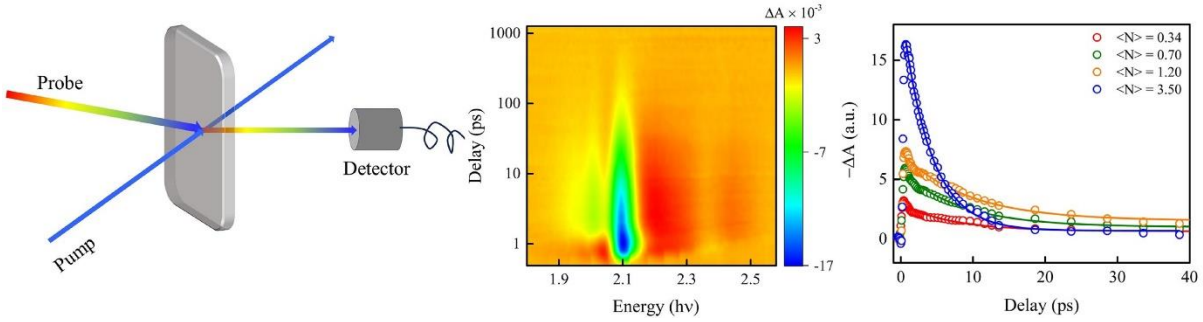

Figure 1: *From right to left*; pump-probe technique, 2D contour plot and calculated Auger recombination time.

References:

1. H. Baker, C. M. Perez, C. Sonnichsen, D. Strandell, O. V. Prezhdo, and P. Kambhampati, ACS Nano, 17 (2023) 3913.
2. A. Dutta, R. K. Behera, P. Pal, S. Baitalik, and N. Pradhan, Angew. Chem. Int. Ed., 58 (2019) 5552.
3. Y. Yang, D. P. Ostrowski, R. M. France, K. Zhu, J. Van De Lagemaat, J. M. Luther, and M. C. Beard, Nat. Photonics., 10 (2016) 53.
4. K. Miyata, D. Meggiolaro, M. T. Trinh, P. P. Joshi, E. Mosconi, S. C. Jones, F. De Angelis, and X.-Y. Zhu, Sci. Adv., 3 (2017) e1701217.